High Power Laser Science and Engineering, (2018), Vol. 6, e41, 5 pages.

doi:10.1017/hpl.2018.35

Variation of the band structure in DKDP crystal excited by intense sub-picosecond laser pulses

Xiaocong Peng[1,2], Yuanan Zhao[1,3], Yueliang Wang[1,2,4], Zhen Cao[1,2], Guohang Hu[1], and Jianda Shao[1]

[1]*Laboratory of Thin Film Optics, Key Laboratory of Materials for High Power Laser, Shanghai Institute of Optics and Fine Mechanics, Chinese Academy of Sciences, Shanghai 201800, China*

[2]*University of Chinese Academy of Sciences, Beijing 100049, China*

[3]*State Key Laboratory of Applied Optics, Changchun Institute of Optics, Fine Mechanics and Physics, Chinese Academy of Sciences, Changchun 130033, China*

[4]*National Engineering Laboratory for Modern Materials Surface Engineering Technology, Guangdong Institute of New Materials, Guangzhou 510650, China*

(Received 4 February 2018; revised 5 May 2018; accepted 14 May 2018)

Abstract

The nonlinear absorption (NLA) properties of potassium dideuterium phosphate crystals at 515 nm under different excitation laser intensities are investigated with the Z-scan technique. Two critical intensities are highlighted: the critical intensity for exciting the NLA and the critical intensity of the multiphoton absorption mechanism transition. Experimental results indicate the existence of defect states located in the band gap, which can be manipulated by varying laser intensity. A model based on the change of multiphoton absorption mechanism induced by the transformation of defect species is proposed to interpret the experiments. Modeling results are in good agreement with the experiment data.

Keywords: multiphoton processes; nonlinear optical materials; Z-scan technique

1. Introduction

Potassium dihydrogen phosphate (KDP) and its deuterated analog, potassium dideuterium phosphate (DKDP) crystals are remarkable multifunctional crystal materials, which are widely applied in fields such as frequency conversion, electro-optic modulation and optical rapid switches[1]. However, the crystal performance is limited due to the unwanted optical absorption, which is attributed to point defects created during crystal growth or generated by irradiation[2–7]. Understanding the role played by point defects in bulk crystals has been a subject of great interest and importance for improving quality and performance of the material[8, 9]. Several theoretical and experimental studies have suggested that point defects in bulk crystals can provide states in the band gap[8–11] and assist in the multiphoton absorption process[12–16].

Throughout the literature, some models have been proposed for understanding the effect of defect states on the nonlinear absorption (NLA) properties of KDP/DKDP crystals. Demos *et al.* proposed that defects induced two electronic states in the band gap that facilitated excitation of valence electrons to the conduction band (CB) through sequential one-photon absorption events at 355 nm and (1 + 2 + 1)-photon absorption (PA) at 532 nm[13]. Duchateau *et al.* also developed a model with two defect states in the band gap, which reduced the order of the multiphoton process to interpret the physical mechanisms of two relaxation dynamics in the KDP/DKDP crystals at 800 nm[14]. However, defect states located in the band gap may change under laser irradiation since they can be produced or eliminated with the addition or removal of electrons[8–11] and subsequently induce changes in the NLA properties of KDP/DKDP crystals[2–4]. The NLA properties of DKDP crystals have been characterized by some authors with the picosecond Z-scan method[17, 18]. However, these experiments were performed under low laser irradiation intensities. In this work, we have carried out studies on the NLA properties of DKDP crystals in the sub-picosecond time scale, allowing us to perform Z-scan experiments with much higher laser intensities and observe possible changes. A model based on the change of multiphoton absorption mechanism induced by the transformation of defect species is proposed to interpret the experimental data.

Correspondence to: Y. Zhao and J. Shao, No. 390 Qinghe Road, Jiading, Shanghai 201800, China. Email: yazhao@siom.ac.cn (Y. Zhao), jdshao@mail.shcnc.ac.cn (J. Shao)

2. Experimental setup

The NLA properties of the samples were investigated by an open-aperture (OA) Z-scan system[19–21]. The pump source of the Z-scan system was a mode-locked fiber laser with a wavelength of 1030 nm (pulse duration of 340 fs and repetition rate of 1 kHz). The NLA of the sample was investigated at a second harmonic wavelength, 515 nm, with a photon energy $\hbar\omega = 2.41$ eV. The pump beam was focused on the sample with a minimum beam waist radius of $\sim$12.5 μm through a lens with a focal length of 15 cm. The sample investigated in this study was a type-II cut DKDP crystal (70% deuteration level) grown by the conventional method. The sample was cut into 30 mm × 30 mm × 0.5 mm dimensions and polished to optical quality. The thickness of the sample ($L = 0.5$ mm) was less than the Rayleigh length ($z_0 = 1$ mm).

3. Results and discussion

To determine the NLA properties of the sample, the Z-scan experiments were performed at different laser intensities (I_{00}) adjusted by rotating the neutral density filter. Note that I_{00} is the on-axis peak intensity at the focus point. Since the band gap value of DKDP crystals is close to 7.8 eV[12], four photons would be required to make an electron transition from the valence band (VB) to the CB. The four-photon absorption (4PA) theory[22] was used to fit the Z-scan results, where the value of linear absorption coefficient was calculated from the linear transmittance measured by a spectrophotometer (PE Lambda 1050) and evaluated to be 0.196 cm^{-1}. As shown in Figure 1, the NLA phenomenon was observed at $I_{00} = 338.05$ GW/cm^2, but not observed at $I_{00} = 270.44$ GW/cm^2, and the NLA coefficient remained nearly constant. Therefore, the critical intensity for exciting the NLA (denoted as I_c) was between $I_{00} = 270.44$ GW/cm^2 and $I_{00} = 338.05$ GW/cm^2. Here we roughly took $I_c = 338.05$ GW/cm^2. The 4PA coefficient α_4 was of the order of $\sim 10^{-8}$ cm^5/GW^3, and the corresponding 4PA cross section σ_{4PA} was determined to be $\sim 10^{-110}$ cm$^8 \cdot$ s^3 by $\sigma_{4PA} = (\hbar\omega)^3\alpha_4/N_0$, where $N_0 = 5 \times 10^{19}$ cm^{-3} is the initial defect density[13]. This value is four orders of magnitude larger than the representative value in wide band gap ideal materials, which is of the order of 10^{-114} cm$^8 \cdot$ s^3[12, 23]. This indicates that the NLA process is not a pure 4PA process; a defect-state-assisted 4PA process may be present.

The OA Z-scan trace displays a symmetric valley with respect to the focus, as shown in Figure 1. However, at an excitation intensity $I_{00} = 1.4I_c$ (denoted as I_{tc}), the symmetric valley changes, as shown in Figure 2. The Z-scan trace can be divided into three parts: (i) the transmittance first drops slowly along the Z direction; (ii) then the transmittance

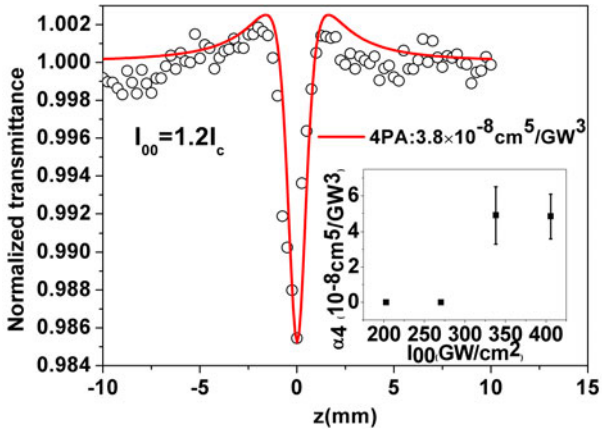

Figure 1. Representative OA Z-scan trace for the DKDP crystal at an excitation intensity of $1.2I_c$. The circular symbols represent the experimental data, while the solid line is the theoretical fitting result by the use of the 4PA theory. The inset is the 4PA coefficient of the DKDP crystal at different excitation laser intensities, while the error bars are the standard deviation from five Z-scan experiments.

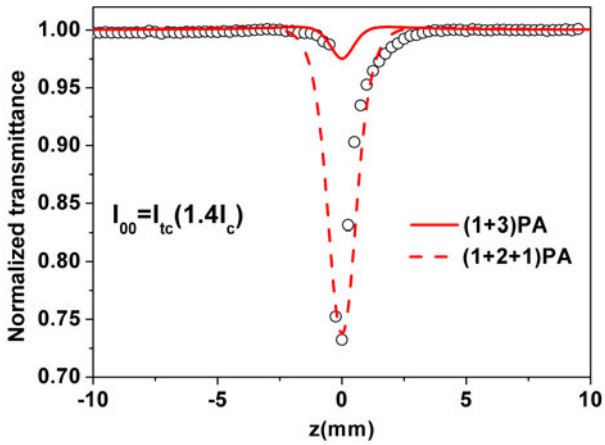

Figure 2. Representative OA Z-scan trace for the DKDP crystal at the excitation intensity of $I_{00} = I_{tc}$. The circular symbols are the experimental data, while the solid (dotted) line is the theoretical fitting result by the use of the $(1 + 3)$ PA theory ($(1 + 2 + 1)$ PA theory).

experiences a sharp drop near the focus point; (iii) the transmittance then rises slowly away from the focus point. The numerical simulation using the 4PA theory cannot fit the whole dataset well. It seems that there is a change of multiphoton absorption mechanism during this process. The $(1+3)$ PA theory and $(1+2+1)$ PA theory mentioned below can fit well with the left and right data, respectively.

Moreover, as shown in Figure 3, after the site is excited with intensity I_{tc}, the phenomenon of NLA becomes more pronounced, and the change lingers for a long time. Furthermore, the phenomenon of NLA can be observed at excitation intensities below I_c after the site is excited with intensity I_{tc}.

The previous results allow for the formation of a hypothesis about the NLA properties of the DKDP crystal

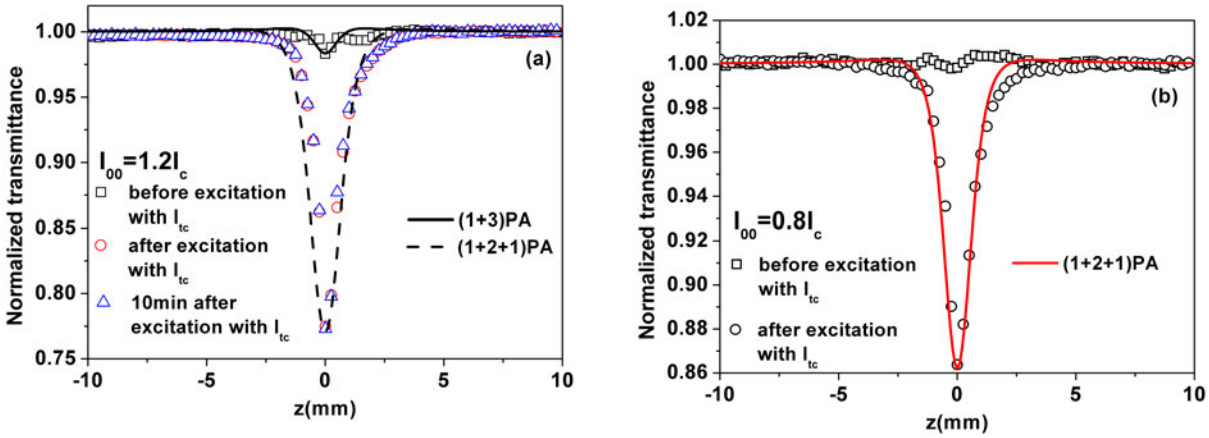

Figure 3. (a) The OA Z-scan traces for the DKDP crystal at the excitation intensity of $I_{00} = 1.2I_c$. Squares, circles and triangles are the experimental data before excitation with I_{tc}, after excitation with I_{tc} and about 10 min after excitation with I_{tc}, respectively. The solid (dotted) line is the theoretical fitting result using the $(1 + 3)$ PA theory ($(1 + 2 + 1)$ PA theory). (b) The OA Z-scan traces for the DKDP crystal at $I_{00} = 0.8I_c$. Squares and circles are the experimental data before excitation with I_{tc} and after excitation with I_{tc}, respectively. The solid line is the theoretical fitting result obtained using the $(1 + 2 + 1)$ PA theory.

at different laser intensities. The cluster of point defects introduces defect states in the band gap, which reduces the multiphoton order required to promote valance electrons to the CB. For a fresh site, the NLA process occurs only when the excitation intensity exceeds I_c, and this process is a defect-state-assisted multiphoton absorption process, in which the electrons transfer into the CB through intraband states. When the site is excited with a higher intensity (larger than I_{tc}), before the focus point, the defect-state-assisted multiphoton absorption process occurs in a similar manner to when the sites were excited by $I_{00} < I_{tc}$. Near the focus point, the laser intensity is very strong and produces new defect states in the band gap. The new defect states further reduce the order of the multiphoton absorption needed for the electron transition. Therefore, the NLA after the focus point is improved. Since this process is not recoverable, the new defect states make the NLA process easier to excite and be observed at excitation intensities below I_c. The observed I_{tc} can be understood as the critical intensity of the multiphoton absorption mechanism transition.

To confirm the above-mentioned analysis and further interpret the experimental data, we propose a model based on the change of multiphoton absorption mechanism induced by the transformation of defect species. We assume that the DKDP crystal undergoes a $(1 + 3)$ PA process before excitation with intensity I_{tc}. Since electronic structure models with two defect states in the band gap proposed by Demos *et al.* and Duchateau *et al.* can interpret some experimental results well[13, 14], we combine their analysis of the possible location of the defect states, and consider that a new defect state located in the band gap is produced after excitation with intensity I_{tc} followed by the $(1 + 2 + 1)$ PA process, as shown in Figure 4. A possible example of the transformation of defect species is an oxygen vacancy. After

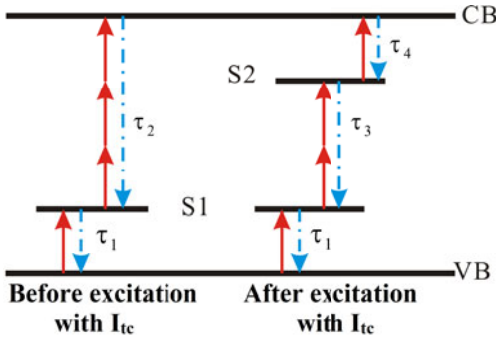

Figure 4. Schematic illustration of the band structure. The solid arrows indicate the absorption of photons, whereas the dash-dotted arrows indicate the relaxation process. S1 and S2 are the states located in the band gap.

excitation with intensity I_{tc}, a large number of electrons and holes are produced. Some of the holes can be trapped at neutral O vacancies and lead to the production of +1 charged O vacancies[24]. The defect is transformed from a neutral O vacancy, which provides only one state in the band gap, into a +1 charged O vacancy, which can provide two states[11].

The attenuation of the pulse intensity as light propagates through the sample can be described as follows.

Before excitation with intensity I_{tc}:

$$\frac{\partial I}{\partial z'} = -\sigma_1 I n_0 - \frac{\sigma_3}{(\hbar\omega)^2} I^3 n_1. \tag{1}$$

After excitation with intensity I_{tc}:

$$\frac{\partial I}{\partial z'} = -\sigma_1 I n_0 - \frac{\sigma_2}{\hbar\omega} I^2 n_1 - \sigma_1' I n_2, \tag{2}$$

where z' is the propagation length inside the sample; σ_1 is the one-photon absorption (1PA) cross section to bridge the VB to S1, σ_1' is the 1PA cross section to bridge S2 to the CB, σ_2 is the two-photon absorption (2PA) cross section to bridge S1 to S2 and σ_3 is the three-photon absorption (3PA) cross section to bridge S1 to the CB; n_0, n_1 and n_2 are the electron densities in the VB, S1 and S2, respectively.

The populations of states can be described by a simple set of rate equations as follows.

Before excitation with intensity I_{tc}:

$$\frac{\partial n_0}{\partial t} = -\sigma_1 \frac{I}{\hbar\omega} n_0 + \frac{n_1}{\tau_1}, \tag{3a}$$

$$\frac{\partial n_1}{\partial t} = \sigma_1 \frac{I}{\hbar\omega} n_0 - \sigma_3 \left(\frac{I}{\hbar\omega}\right)^3 n_1 + \frac{n_{cb}}{\tau_2} - \frac{n_1}{\tau_1}, \tag{3b}$$

$$\frac{\partial n_{cb}}{\partial t} = \sigma_3 \left(\frac{I}{\hbar\omega}\right)^3 n_1 - \frac{n_{cb}}{\tau_2}, \tag{3c}$$

$$n = n_0 + n_1 + n_{cb}. \tag{3d}$$

After excitation with intensity I_{tc}:

$$\frac{\partial n_0}{\partial t} = -\sigma_1 \frac{I}{\hbar\omega} n_0 + \frac{n_1}{\tau_1}, \tag{4a}$$

$$\frac{\partial n_1}{\partial t} = \sigma_1 \frac{I}{\hbar\omega} n_0 - \sigma_2 \left(\frac{I}{\hbar\omega}\right)^2 n_1 + \frac{n_2}{\tau_3} - \frac{n_1}{\tau_1}, \tag{4b}$$

$$\frac{\partial n_2}{\partial t} = \sigma_2 \left(\frac{I}{\hbar\omega}\right)^2 n_1 - \sigma_1' \frac{I}{\hbar\omega} n_2 + \frac{n_{cb}}{\tau_4} - \frac{n_2}{\tau_3}, \tag{4c}$$

$$\frac{\partial n_{cb}}{\partial t} = \sigma_1' \frac{I}{\hbar\omega} n_2 - \frac{n_{cb}}{\tau_4}, \tag{4d}$$

$$n = n_0 + n_1 + n_2 + n_{cb}, \tag{4e}$$

where τ_1, τ_2, τ_3 and τ_4 are the relaxation times of S1 to the VB, the CB to S1, S2 to S1 and the CB to S2, respectively; n and n_{cb} are the initial electron density in the VB and electron density in the CB, respectively. The value of n_{cb} is close to zero at relatively low energy excitation conditions since the electrons pumped onto the CB jump back promptly due to the short relaxation time from the CB to the defect state. In this analysis, we emphasize that the transition only takes place in the vicinity of the defects and assume that the VB is not sufficiently depleted for the light excitations used in the model. Therefore $n_1 \ll n$, $n_2 \ll n$; we set $n_0 \approx n = N_0$. Under the excitation of the ultrafast laser with a spatial and temporal Gaussian profile, we have $I = I_0 \exp(-t^2/\tau^2)$, where I_0 gives the spatial profile and τ is the pulse width. Considering that τ_1 is of the order of 1 ns or shorter and τ_3 is of the picosecond time scale (τ is much smaller than the relaxation times)[13], the population densities of S1 and S2 are as follows.

Before excitation with intensity I_{tc}:

$$n_1 = \frac{\sigma_1 n}{\hbar\omega} \int_{-\infty}^{t} I(t')\, \mathrm{d}t'. \tag{5}$$

Table 1. Value of the parameters used in the fitting.

Symbol	Value	Comment
σ_1	2.3×10^{-19} cm^2	1PA cross section
σ_1'	6.4×10^{-17} cm^2	1PA cross section
σ_2	2.0×10^{-48} cm$^4 \cdot$ s	2PA cross section
σ_3	6.1×10^{-79} cm$^6 \cdot$ s^2	3PA cross section

After excitation with intensity I_{tc}:

$$n_1 = \frac{\sigma_1 n}{\hbar\omega} \int_{-\infty}^{t} I(t') \exp\left\{\sigma_2 \left(\frac{I_0}{\hbar\omega}\right)^2 \frac{\sqrt{2\pi}\tau}{4} \left[\mathrm{erf}\left(\frac{\sqrt{2}t'}{\tau}\right) - \mathrm{erf}\left(\frac{\sqrt{2}t}{\tau}\right)\right]\right\} \mathrm{d}t', \tag{6a}$$

$$n_2 = \frac{\sigma_2}{(\hbar\omega)^2} \int_{-\infty}^{t} n_1 I^2(t')\, \mathrm{d}t', \tag{6b}$$

where $\mathrm{erf}(x)$ is the error function.

We could revise Equations (1) and (2) with the space and time average approximation method[25, 26] as

$$\frac{\partial I}{\partial z'} = -\sigma_1 n I - \sqrt{\frac{\pi}{3}} \frac{\sigma_3 \sigma_1 n \tau}{(\hbar\omega)^3} I^4, \tag{7}$$

$$\frac{\partial I}{\partial z'} = -\sigma_1 n I - \frac{\sigma_2 \sigma_1 n}{(\hbar\omega)^2} A I^3 - \frac{\sigma_1' \sigma_2 \sigma_1 n}{(\hbar\omega)^3} B I^4, \tag{8}$$

where

$$A = \frac{\sqrt{3}\tau \int_{-\infty}^{+\infty} \int_{-\infty}^{y} \int_{0}^{L} \int_{0}^{+\infty} F \mathrm{d}r\, \mathrm{d}z\, \mathrm{d}x\, \mathrm{d}y}{\sqrt{\pi} \int_{0}^{L} \int_{0}^{+\infty} r I_0^3 \mathrm{d}r\, \mathrm{d}z}, \tag{9a}$$

$$B = \frac{2\tau^2 \int_{-\infty}^{+\infty} \int_{-\infty}^{Q} \int_{-\infty}^{y} \int_{0}^{L} \int_{0}^{+\infty} I_0 F \exp(-Q^2)\, \mathrm{d}r\, \mathrm{d}z\, \mathrm{d}x\, \mathrm{d}y\, \mathrm{d}Q}{\sqrt{\pi} \int_{0}^{L} \int_{0}^{+\infty} r I_0^4 \mathrm{d}r\, \mathrm{d}z}, \tag{9b}$$

$$F = r I_0^3 \exp\left\{\sigma_2 \left(\frac{I_0}{\hbar\omega}\right)^2 \frac{\sqrt{2\pi}\tau}{4} [\mathrm{erf}(\sqrt{2}x) - \mathrm{erf}(\sqrt{2}y)] - 2y^2 - x^2\right\}. \tag{9c}$$

Equation (7) is formally consistent with the light propagation equation which describes the 4PA process in the sample. Equation (8) is formally consistent with the light propagation equation which describes the concurrence of 3PA process and 4PA process in the sample. Therefore, we can use the results from Ref. [22] to fit our experimental data. As can be seen in Figures 2 and 3, the fit lines are in good agreement with the experimental data. For the entire range of intensities, the best fit of the experimental data is obtained with the parameter values summarized in Table 1. The obtained generalized multiphoton absorption cross sections are comparable to the empirical formula[27].

4. Conclusions

In summary, based on the Z-scan technique, the NLA properties of the DKDP crystal at 515 nm under different excitation laser intensities were investigated. This study has shown that two critical intensities exist: (i) the critical intensity (I_c) for exciting the NLA (as the intensity exceeds I_c, 4PA is observed and the absorption cross section is larger than the representative value in wide band gap ideal materials); (ii) the critical intensity (I_{tc}) of the multiphoton absorption mechanism transition (after the site is excited with an intensity larger than I_{tc}, the phenomenon of NLA is enhanced and can be observed below the I_c value). The experimental data are supported by a model based on the change of multiphoton absorption mechanism induced by the transformation of defect species, which can provide a different number of states in the band gap. These results clearly show the existence of defect states in the band gap, which can assist in multiphoton absorption and be manipulated by varying laser intensity.

Acknowledgement

This work is supported by the National Natural Science Foundation of China (Nos. 61405219 and 11304328).

References

1. D. Eimerl, Ferroelectrics **72**, 95 (1987).
2. J. E. Davis, R. S. Hughes, and H. W. H. Lee, Chem. Phys. Lett. **207**, 540 (1993).
3. C. D. Marshall, S. A. Payne, M. A. Henesian, J. A. Speth, and H. T. Powell, J. Opt. Soc. Am. B **11**, 774 (1994).
4. S. G. Demos, M. Staggs, and H. B. Radousky, Phys. Rev. B **67**, 224102 (2003).
5. Y. B. Zheng, L. Ding, X. D. Zhou, R. S. Ba, J. Yuan, H. L. Xu, X. Y. Yang, B. Chen, J. Na, Y. J. Li, and W. G. Zheng, Chin. Opt. Lett. **14**, 051601 (2016).
6. M. M. Chirila, N. Y. Garces, L. E. Halliburton, S. G. Demos, T. A. Land, and H. B. Radousky, J. Appl. Phys. **94**, 6456 (2003).
7. I. N. Ogorodnikov, V. Yu. Yakovlev, B. V. Shul'gin, and M. K. Satybaldieva, Phys. Solid State **44**, 880 (2002).
8. K. P. Wang, C. S. Fang, J. X. Zhang, C. S. Liu, R. I. Boughton, S. L. Wang, and X. Zhao, Phys. Rev. B **72**, 184105 (2005).
9. C. S. Liu, N. Kioussis, S. G. Demos, and H. B. Radousky, Phys. Rev. Lett. **91**, 015505 (2003).
10. C. S. Liu, Q. Zhang, N. Kioussis, S. G. Demos, and H. B. Radousky, Phys. Rev. B **68**, 224107 (2003).
11. C. S. Liu, C. J. Hou, N. Kioussis, S. G. Demos, and H. B. Radousky, Phys. Rev. B **72**, 134110 (2005).
12. C. W. Carr, H. B. Radousky, and S. G. Demos, Phys. Rev. Lett. **91**, 127402 (2003).
13. S. G. Demos, P. DeMange, R. A. Negres, and M. D. Feit, Opt. Express **18**, 13788 (2010).
14. G. Duchateau, G. Geoffroy, A. Dyan, H. Piombini, and S. Guizard, Phys. Rev. B **83**, 075114 (2011).
15. G. Duchateau, M. D. Feit, and S. G. Demos, J. Appl. Phys. **111**, 093106 (2012).
16. G. Duchateau, G. Geoffroy, A. Belsky, N. Fedorov, P. Martin, and S. Guizard, J. Phys. Condens. Matter **25**, 435501 (2013).
17. D. L. Wang, S. L. Wang, J. Y. Wang, C. Y. Shen, W. D. Li, P. P. Huang, H. Liu, and R. I. Boughton, Crystals **7**, 188 (2017).
18. D. L. Wang, T. B. Li, S. L. Wang, J. Y. Wang, C. Y. Shen, J. X. Ding, W. D. Li, P. P. Huang, and C. W. Lu, Opt. Mater. Express **7**, 533 (2017).
19. M. Sheik-Bahae, A. A. Said, T. H. Wei, D. J. Hagan, and E. W. Van Stryland, IEEE J. Quantum Electron **26**, 760 (1990).
20. J. Wang, D. Früchtl, Z. Y. Sun, J. N. Coleman, and W. J. Blau, J. Phys. Chem. C **114**, 6148 (2010).
21. K. P. Wang, J. Wang, J. T. Fan, M. Lotya, A. O'Neill, D. Fox, Y. Y. Feng, X. Y. Zhang, B. X. Jiang, Q. Z. Zhao, H. Z. Zhang, J. N. Coleman, L. Zhang, and W. J. Blau, ACS Nano **7**, 9260 (2013).
22. B. Gu, X. Q. Huang, S. Q. Tan, M. Wang, and W. Ji, Appl. Phys. B **95**, 375 (2009).
23. S. C. Jones, P. Braunlich, R. T. Casper, X. A. Shen, and P. Kelly, Opt. Eng. **28**, 281039 (1989).
24. S. M. Evans, N. C. Giles, L. E. Halliburton, and L. A. Kappers, J. Appl. Phys. **103**, 043710 (2008).
25. R. L. Sutherland, *Handbook of Nonlinear Optics* (CRC Press, New York, 2003), p. 634.
26. B. Gu and W. Ji, Opt. Express **16**, 10208 (2008).
27. P. Agostini and G. Petite, Contemp. Phys. **29**, 57 (1988).